Jet suppression of pions and single electrons at Au + Au collisions at the BNL Relativistic Heavy Ion Collider

Magdalena Djordjevic
Institute of Physics Belgrade, University of Belgrade, Serbia
(Received 17 June 2011; revised manuscript received 1 September 2011; published 12 March 2012)

Jet suppression is considered to be a powerful tool to study the properties of a QCD medium created in ultrarelativistic heavy ion collisions. However, theoretical predictions obtained by using jet energy loss in a *static* QCD medium show disagreement with experimental data, which is known as the heavy flavor puzzle at Relativistic Heavy Ion Collisider (RHIC). We calculate the suppression patterns of pions and single electrons for Au + Au collisions at RHIC by including the energy loss in a finite size *dynamical* QCD medium, with finite magnetic mass effects taken into account. We here report a notably improved agreement with the experimental results compared to the static case; this agreement is robust with respect to a realistic range of magnetic mass values. Therefore, the inclusion of dynamical QCD medium effects provides an important step toward understanding the heavy flavor puzzle at RHIC.

DOI: 10.1103/PhysRevC.85.034904 PACS number(s): 12.38.Mh, 24.85.+p, 25.75.−q

I. INTRODUCTION

Jet suppression [1] measurements at Relativistic Heavy Ion Collider (RHIC) and Large Hadron Collider (LHC), and their comparison with theoretical predictions, provide a powerful tool for mapping the properties of a QCD medium created in ultrarelativistic heavy ion collisions [2–4]. However, jet suppression predictions, done under the assumption of a static QCD medium [5–7], showed a disagreement with the available data from RHIC experiments [8–11], as they are not able to simultaneously explain *both* pion and single electron suppression data. This disagreement has been named "heavy flavor puzzle at RHIC" [12,13], and raised important questions about the ability of the available theories to model the matter created at ultrarelativistic heavy ion collisions at RHIC. Moreover, this disagreement inspired some theorists to seek explanations outside conventional QCD (see, e.g., Refs. [14–17]).

Before considering solutions outside perturbative QCD (pQCD), it is useful to note that—from the Quark Gluon Plasma (QGP) point of view—the jet suppression results from the energy loss of high energy partons moving through the plasma [18–21]. Therefore, accurate computations of jet energy loss mechanisms are essential for the reliable predictions of jet suppression. However, all available energy loss models [22–28], which can treat both light and heavy quark jets, were based on the assumption of a static QCD medium [5–7], where interactions are modeled as static color-screened Yukawa potentials [24]. Since, in reality, the scattering centers are dynamical, it is evident that such an approximation does not provide a realistic description of the QCD medium created in ultrarelativistic heavy ion collisions. With this goal, in Refs. [29,30], we developed a theoretical formalism[1] for the calculation of radiative energy loss in a realistic finite size *dynamical* QCD medium (see also Ref. [12]), which abolished a static approximation used in previous models [22–28]. Furthermore, in Ref. [31], we extended the study from Ref. [29] to include the possibility for the existence of finite magnetic mass; this generalization was motivated by various nonperturbative approaches [32–35], which report nonzero magnetic mass. These studies, together with the previously developed collisional energy loss formalism in finite size dynamical QCD medium [36], enable us to provide the most reliable computations of the energy loss in QGP so far.

In this paper, we integrate the developed energy loss formalism into a computational framework that can generate reliable predictions for RHIC and LHC experimental data. The numerical procedure includes: (i) both collisional and radiative energy loss from the newly developed (dynamical QCD medium) formalism [29–31,36], (ii) multigluon fluctuations (i.e., the fact that energy loss is a distribution [37]), and (iii) path length fluctuations (i.e., the fact that particles travel different paths in the medium [38]). We use this framework to generate suppression predictions for pions and single electrons at most central 200 GeV Au + Au collisions at RHIC. The generated predictions are directly compared with RHIC experimental data [8–11] to test our understanding of QGP created at these collisions.

II. COMPUTATIONAL FRAMEWORK

The quenched spectra of partons, hadrons, and leptons are calculated as in Refs. [5,38] from the generic pQCD convolution

$$\frac{E_f d^3\sigma(e)}{dp_f^3} = \frac{E_i d^3\sigma(Q)}{dp_i^3} \otimes P(E_i \to E_f) \otimes D(Q \to H_Q) \otimes f(H_Q \to e), \quad (1)$$

where Q denotes quarks and gluons. For charm and bottom, the initial quark spectrum, $E_i d^3\sigma(Q)/dp_i^3$, is computed at next-to-leading order using the code from Refs. [39,40]; for gluons and light quarks, the initial distributions are computed at leading order as in Ref. [41] (see also Ref. [42]). $P(E_i \to E_f)$ is

[1]The dynamical energy loss formalism is based on calculating 24 Feynman diagrams through the hard thermal loop (HTL) approach, and applies to the case of a finite, optically thin QCD medium.

the energy loss probability, $D(Q \to H_Q)$ is the fragmentation function of quark or gluon Q to hadron H_Q. The last step $[f(H_Q \to e)]$ is only applicable for heavy quarks and it represents the decay function of hadron H_Q into the observed single electron. We use the same mass and factorization scales as in Ref. [43] and employ the CTEQ5M parton densities [44] with no intrinsic k_T. As in Ref. [43] we neglect shadowing of the nuclear parton distribution.

We assume that the final quenched energy E_f is large enough that the Eikonal approximation can be employed. We also assume that in Au + Au collisions, the jet to hadron fragmentation functions are the same as in e^+e^- collisions. This assumption is expected to be valid in the deconfined medium case, where the hadronization of $Q \to H_Q$ cannot occur until the quark emerges from the QGP.

As in Ref. [38], the energy loss probability $P(E_i \to E_f)$ is generalized to include both radiative and collisional energy loss and their fluctuations. However, while the authors of Ref. [38] assumed a static QCD medium, the present study takes into account both the radiative [29] and collisional [36] energy losses in a realistic *finite size dynamical* QCD medium.

To take into account geometric path length fluctuations in the energy loss probability, we use [38]

$$P\ (E_i \to E_f = E_i - \Delta_{\rm rad} - \Delta_{\rm coll}) = \int dL\ P(L)\ P_{\rm rad}(\Delta_{\rm rad}; L) \otimes P_{\rm coll}(\Delta_{\rm coll}; L). \quad (2)$$

Here $P(L)$ is the distribution of the path lengths traversed by hard scatterers in 0–5% of most central collisions, in which the lengths are weighted by the probability of production and averaged over azimuth. Note that currently two definitions for $P(L)$ (see Ref. [45]), one from Ref. [38] and the other from Ref. [46], are commonly used. Since these distributions are significantly different (see Fig. 1, where these distributions are graphically represented), we will use both of them in the analysis. Also, since $P(L)$ is a purely geometric quantity, it is the same for all jet varieties.

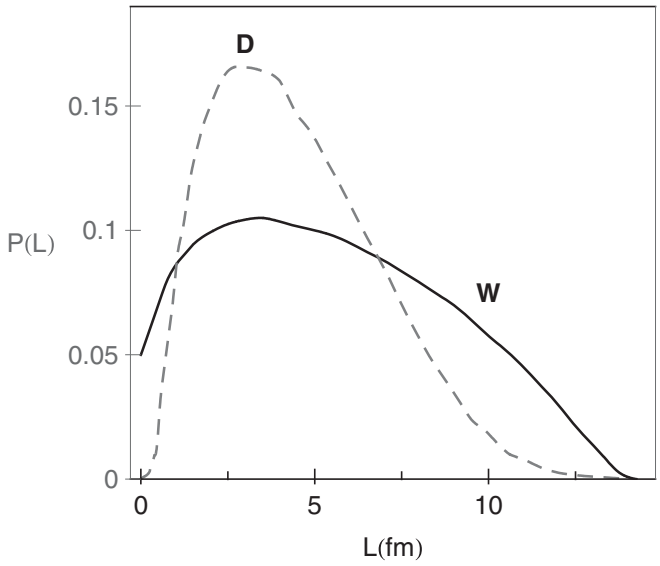

FIG. 1. Path length distributions that are used for the suppression calculations. The solid curve corresponds to the distribution used in Ref. [38] (marked with "W"), while the dashed curve corresponds to the distribution used in Ref. [46] (marked with "D").

$P_{\rm rad}(\Delta_{\rm rad}; L)$ and $P_{\rm coll}(\Delta_{\rm coll}; L)$ in Eq. (2) are, respectively, the radiative and collisional energy loss probabilities. The procedure for including fluctuations of the radiative energy loss probability $[P_{\rm rad}(\Delta_{\rm rad}; L)]$ due to gluon number fluctuations is discussed in detail in Refs. [5,47]. Note that the procedure is here generalized to include the radiative energy loss in finite size dynamical QCD medium [29,30], as well as a possibility for existence of finite magnetic mass [31]; in particular, the medium induced gluon radiation spectrum is given by (see Ref. [31])

$$\frac{dN_{\rm rad}}{dx} = \frac{2}{x}\frac{C_R\alpha_s}{\pi}\frac{L}{\lambda_{\rm dyn}}\int\frac{d^2k}{\pi}\frac{d^2q}{\pi}\frac{\mu_E^2-\mu_M^2}{(\boldsymbol{q}^2+\mu_M^2)(\boldsymbol{q}^2+\mu_E^2)} \times\left(1-\frac{\sin\frac{(\boldsymbol{k}+\boldsymbol{q})^2+\chi}{xE^+}L}{\frac{(\boldsymbol{k}+\boldsymbol{q})^2+\chi}{xE^+}L}\right)\frac{(\boldsymbol{k}+\boldsymbol{q})}{(\boldsymbol{k}+\boldsymbol{q})^2+\chi} \times\left(\frac{(\boldsymbol{k}+\boldsymbol{q})}{(\boldsymbol{k}+\boldsymbol{q})^2+\chi}-\frac{\boldsymbol{k}}{\boldsymbol{k}^2+\chi}\right). \quad (3)$$

Here L is the length of the finite size dynamical QCD medium and E is the jet energy. μ_E is the Debye mass (electric screening) and μ_M is magnetic screening. $\boldsymbol{k}$ is the transverse momentum of radiated gluon, while $\boldsymbol{q}$ is the transverse momentum of the exchanged (virtual) gluon. $v(\boldsymbol{q})$ is the effective cross section in a dynamical QCD medium and $\lambda_{\rm dyn}^{-1} \equiv C_2(G)\alpha_s T = 3\alpha_s T$ $[C_2(G) = 3]$ is defined as the "dynamical mean free path" [48]. $\alpha_s = \frac{g^2}{4\pi}$ is the coupling constant and $C_R = \frac{4}{3}$. $\chi \equiv M^2x^2 + m_g^2$, where x is the longitudinal momentum fraction of the heavy quark carried away by the emitted gluon, and $m_g = \mu_E/\sqrt{2}$ is the effective mass for gluons with hard momenta $k \gtrsim T$ [49].

For collisional energy loss probability $[P_{\rm coll}(\Delta_{\rm coll}; L)]$, the full fluctuation spectrum is approximated by a Gaussian centered at the average energy loss with variance $\sigma^2_{\rm coll} = 2T\langle\Delta E^{\rm coll}(p_\perp, L)\rangle$ [38,50]. Here $\Delta E^{\rm coll}(p_\perp, L)$ is extracted from Ref. [36], T is the temperature of the medium, $p_\perp$ is the initial momentum of the jet, and L is the length of the medium traversed by the jet.

We note that, in the suppression calculations, we separately treat radiative from collisional energy loss. Consequently, we first calculate the modification of the quark and gluon spectrum due to radiative energy loss, and then due to collisional energy loss in the QCD medium. This is a reasonable approximation when the radiative and collisional energy losses can be considered small (which is in the essence of the soft-gluon, soft-rescattering approximation used in all energy loss calculations so far [22–30,51]), and when collisional and radiative energy loss processes are decoupled from each other (which is the case in the HTL approach [52] used in our energy loss calculations [29,30,36]). Also, we assume that the strong coupling constant α_S is fixed at 0.3, which is considered to approximate well the coupling at RHIC [53–55].

Finally, to obtain π^0 suppression from quark and gluon suppression, we use the following approximation [56,57]

$$R_{AA}(\pi^0, p_\perp) \approx f_g R_{AA}(g, p_\perp) + (1 - f_g)R_{AA}(l, p_\perp), \quad (4)$$

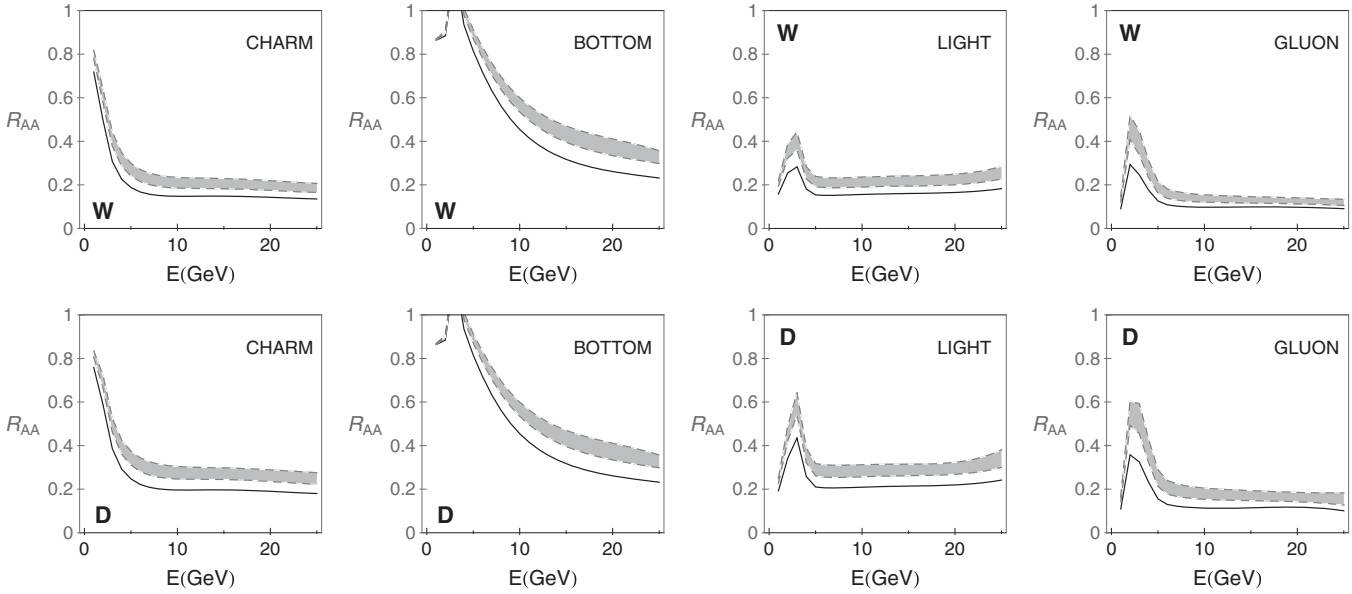

FIG. 2. Quarks and gluon suppressions are presented as a function of initial jet energy for 200 GeV Au + Au collisions at RHIC. The upper four panels and the lower four panels are obtained, respectively, by using the path length distributions from Ref. [38] (marked with "W") and Ref. [46] (marked with "D"). On each panel, the solid curves correspond to zero magnetic mass. The gray bands correspond to nonzero magnetic mass (i.e., $0.4 < \mu_M/\mu_E < 0.6$ [32–35]), where the lower boundary corresponds to $\mu_M/\mu_E = 0.4$ and the upper boundary corresponds to $\mu_M/\mu_E = 0.6$.

where $f_g \approx e^{-p_\perp/10.5\,\mathrm{GeV}}$ is the fraction of pions with a given momentum $p_\perp$ that arise from gluon jet fragmentation, $R_{AA}(g, p_\perp)$ is the gluon suppression, and $R_{AA}(l, p_\perp)$ is the light quark suppression.

To calculate D and B meson suppression, we will use both delta and Peterson [58] fragmentation functions. Furthermore, the single electron suppression is obtained according to the analysis presented in Ref. [5].

III. NUMERICAL RESULTS

In this section, we concentrate at 200 GeV Au + Au collisions at RHIC, and present our suppression predictions for light and heavy flavor observables. For this, we consider a quark-gluon plasma of temperature $T = 225$ MeV, with $N_f = 2.5$ effective light quark flavors and strong interaction strength $\alpha_S = 0.3$, as representative of average conditions encountered in Au + Au collisions at RHIC. For the light quarks we assume that their mass is dominated by the thermal mass $M = \mu/\sqrt{6}$, where $\mu = gT\sqrt{1+N_f/6} \approx 0.5$ GeV is the Debye screening mass. The gluon mass is taken to be $m_g = \mu/\sqrt{2}$. For the charm (bottom) mass we use $M = 1.2$ GeV ($M = 4.75$ GeV).

Figure 2 shows the momentum dependence of quarks and gluon suppressions at RHIC, obtained by using two path length distributions from Ref. [38] and from Ref. [46]. For both path length distributions, we observe a clear hierarchy between the quarks and gluon suppressions: (i) the bottom quark is significantly less suppressed than the charm quark; (ii) the charm and light quarks have similar suppressions for initial jet energies larger than 5 GeV; (iii) gluons are significantly more suppressed than all types of quarks. This already observed/established hierarchy (see, e.g., Ref. [47]) therefore remains valid for the case of the dynamical QCD medium as well, despite the fact that both the inclusion of path length fluctuations [38] and dynamical effects [30] into the suppression calculations tend to reduce the difference between different types of quarks and gluons. We also observe that the inclusion of magnetic mass can decrease the jet suppression (for all types of quarks and gluons) for 25–50%, compared to the case of zero magnetic mass. Regarding different path length distributions, we observe somewhat lower suppression results

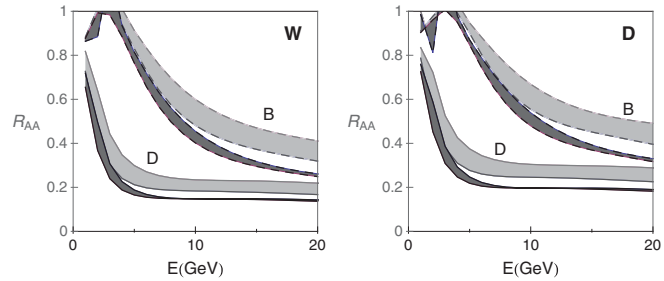

FIG. 3. Suppressions of D and B mesons are shown as a function of initial jet energy. The left and the right panels are obtained, respectively, by using path length distributions from Ref. [38] (marked with "W") and Ref. [46] (marked with "D"). On each panel, the bands with solid and dashed boundaries correspond to, respectively, D and B mesons. Also, on each panel, the dark gray bands correspond to zero magnetic mass, while light gray bands correspond to nonzero magnetic mass (i.e., $0.4 < \mu_M/\mu_E < 0.6$ [32–35]). The upper and the lower boundaries of each band are obtained by using, respectively, Peterson [58] and delta fragmentation functions.

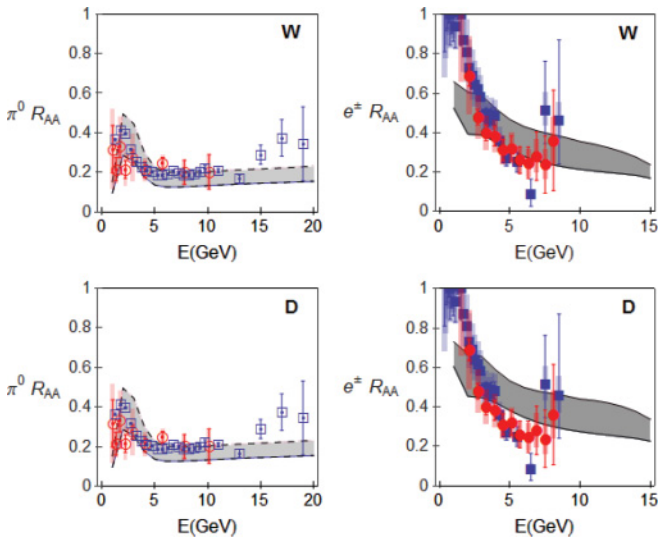

FIG. 4. (Color online) The left panels show the comparison of the pion suppression predictions with π^0 PHENIX [8] (shown in blue) and STAR [10] (shown in red) experimental data from 200 GeV Au + Au collisions at RHIC. The right panels show the comparison of the single electron suppression predictions with the non-photonic single electron data from PHENIX [9] (shown in blue) and STAR [11] (shown in red) at 200 GeV Au + Au collisions. For the two upper panels and the two lower panels the suppression predictions are obtained, respectively, by using the path length distributions from Ref. [38] (marked with "W") and Ref. [46] (marked with "D"). On each panel, the gray region corresponds to the case when $\mu_M \geqslant 0$ (i.e., $0 < \mu_M/\mu_E < 0.6$), where the lower boundary corresponds to $\mu_M/\mu_E = 0$ and the upper boundary corresponds to $\mu_M/\mu_E = 0.6$.

when the distribution from Ref. [46] is used; this is expected keeping in mind the higher probability for lower path lengths in Ref. [46] compared to Ref. [38] (see Ref. [45]).

To calculate D and B meson suppression we use both delta and Peterson [58] fragmentation functions and observe that the choice of fragmentation function only marginally changes the value of suppression R_{AA} (see dark gray bands in Fig. 3). The reason behind the small difference is that fragmentation functions do not significantly modify the distribution slopes [47], due to which the meson suppression becomes insensitive to the choice of fragmentation function. However, for the single electron suppression, the choice of fragmentation function can influence the final suppression result (see Ref. [5]), so we will continue to use both fragmentation functions for the calculation of the single electron suppression.

Figure 4 shows the momentum dependence of pion and single electron suppressions at RHIC, obtained by using the two path length distributions (from Ref. [38] and from Ref. [46]). The predictions are compared with the relevant PHENIX [8,9] and RHIC [10,11] experimental data at Au + Au collisions at RHIC. For both path length distributions we observe a reasonable agreement with the experimental data; this agreement is moreover robust when nonzero magnetic mass is introduced.

Furthermore, from Fig. 4 we see that as the jet energies approach 15 GeV, the predicted pion and single electron suppressions become very similar. This prediction is reasonable since (i) at high jet energies suppression patterns for all types of quarks become similar, and (ii) above 10 GeV pion suppression is strongly dominated by light quark suppression (i.e., gluon contribution to pion suppression becomes negligible) [56,57]. This behavior is qualitatively different from the one below 10 GeV, where the obtained suppressions are notably different (by $\lesssim 2$). It will be interesting to compare this predicted pattern with the upcoming high luminosity RHIC data.

IV. CONCLUSION

A major theoretical problem in relativistic heavy ion physics is the apparent inability of pQCD to consistently explain both pion and single electron data at RHIC, which was termed the "heavy flavor puzzle." This puzzle recently inspired approaches that look for a solution outside of conventional QCD (see, e.g., Refs. [14–17]). The main goal of this paper was to show that considering a more realistic dynamical QCD medium significantly improves the agreement between theoretical predictions and experimental data; this improvement gives confidence that pQCD may still be able to provide a reasonable explanation of both pion and single electron data.

To this end we here calculated the suppression pattern of pions, D and B mesons, and single electrons in central 200 GeV Au + Au collisions at RHIC energies. The calculation is based on the radiative and collisional energy loss in a finite size dynamical QCD medium, which is a key ingredient for obtaining reliable predictions for jet quenching in ultrarelativistic heavy ion collisions. This energy loss formalism was here integrated into a computational framework that includes multigluon and path length fluctuations, as well as a possibility of finite magnetic mass. The introduction of realistic finite size dynamical QCD medium leads to a significantly improved agreement between the generated suppression patterns and experimental data at Au + Au collisions at RHIC, and this agreement is robust with respect to introduction of finite magnetic mass. The improvement strongly suggests that an important deficiency behind the "heavy flavor puzzle" at RHIC is the *static* approximation (i.e., the fact that the dynamical nature of plasma constituents was not taken into account).

However, to solve the heavy flavor puzzle, both theoretical and experimental uncertainties would have to be notably reduced, which may become possible through future studies. Furthermore, the dynamical energy loss formalism, used to generate predictions in this paper, is based on the first order in opacity calculations. An important future goal is to generalize this energy loss to higher orders in opacity, and explore whether/to what extent such generalization would modify the predictions presented in this paper.

ACKNOWLEDGMENTS

This work is supported by a Marie Curie International Reintegration Grant within the seventh European Community Framework Programme (PIRG08-GA-2010-276913) and by the Ministry of Science and Technological Development of the Republic of Serbia, under Projects No. ON171004 and No. ON173052.

[1] J. D. Bjorken: FERMILAB-PUB-82-059-THY (1982).
[2] N. Brambilla *et al*., CERN Yellow Report, CERN-2005-005, Geneva: CERN, 2005.
[3] M. Gyulassy, Lect. Notes Phys. **583**, 37 (2002).
[4] D. d'Enterria and B. Betz, Lect. Notes Phys. **785**, 285 (2010).
[5] M. Djordjevic, M. Gyulassy, R. Vogt, and S. Wicks, Phys. Lett. B **632**, 81 (2006).
[6] R. Rapp, V. Greco, and H. van Hees, Nucl. Phys. A **774**, 685 (2006).
[7] N. Armesto, A. Dainese, C. A. Salgado, and U. A. Wiedemann, Phys. Rev. D **71**, 054027 (2005).
[8] A. Adare *et al*. (PHENIX Collaboration), Phys. Rev. Lett. **101**, 232301 (2008).
[9] A. Adare *et al*. (PHENIX Collaboration), Phys. Rev. Lett. **98**, 172301 (2007).
[10] B. I. Abelev *et al*. (STAR Collaboration), Phys. Rev. C **80**, 044905 (2009).
[11] B. I. Abelev *et al*. (STAR Collaboration), Phys. Rev. Lett. **98**, 192301 (2007).
[12] M. Gyulassy, Phys. **2**, 107 (2009).
[13] M. Djordjevic, J. Phys. G **32**, S333 (2006).
[14] A. Ficnar, J. Noronha, and M. Gyulassy, J. Phys. G **38**, 124176 (2011).
[15] J. Noronha, M. Gyulassy, and G. Torrieri, arXiv:0906.4099.
[16] S. S. Gubser, D. R. Gulotta, S. S. Pufu, and F. D. Rocha, J. High Energy Phys. 10 (2008) 052; P. M. Chesler, K. Jensen, A. Karch, and L. G. Yaffe, Phys. Rev. D **79**, 125015 (2009).
[17] W. A. Horowitz and M. Gyulassy, Phys. Lett. B **666**, 320 (2008); B. Betz, M. Gyulassy, J. Noronha, and G. Torrieri, *ibid*. **675**, 340 (2009).
[18] M. Guylassy, I. Vitev, X. N. Wang, and B. W. Zhang, in *Quark Gluon Plasma 3*, edited by R. C. Hwa and X. N. Wang (World Scientific, Singapore, 2003), p. 123.
[19] R. Baier, Yu. L. Dokshitzer, A. J. Mueller, and D. Schiff, Phys. Rev. C **58**, 1706 (1998).
[20] R. Baier, D. Schiff, and B. G. Zakharov, Ann. Rev. Nucl. Part. Sci. **50**, 37 (2000).
[21] A. Kovner and U. A. Wiedemann, in *Quark Gluon Plasma 3*, edited by R. C. Hwa and X. N. Wang, (World Scientific, Singapore, 2003), p. 192.
[22] M. Djordjevic and M. Gyulassy, Phys. Lett. B **560**, 37 (2003); Nucl. Phys. A **733**, 265 (2004).
[23] M. Gyulassy, P. Levai, and I. Vitev, Nucl. Phys. B **594**, 371 (2001).
[24] M. Gyulassy and X. N. Wang, Nucl. Phys. B **420**, 583 (1994); X. N. Wang, M. Gyulassy, and M. Plumer, Phys. Rev. D **51**, 3436 (1995).
[25] U. A. Wiedemann, Nucl. Phys. B **588**, 303 (2000); **582**, 409 (2000).
[26] E. Wang and X. N. Wang, Phys. Rev. Lett. **87**, 142301 (2001); X. N. Wang and X. F. Guo, Nucl. Phys. A **696**, 788 (2001); X. F. Guo and X. N. Wang, Phys. Rev. Lett. **85**, 3591 (2000).
[27] N. Armesto, C. A. Salgado, and U. A. Wiedemann, Phys. Rev. D **69**, 114003 (2004).
[28] M. Djordjevic, Phys. Rev. C **73**, 044912 (2006).
[29] M. Djordjevic, Phys. Rev. C **80**, 064909 (2009).
[30] M. Djordjevic and U. Heinz, Phys. Rev. Lett. **101**, 022302 (2008).
[31] M. Djordjevic and M. Djordjevic, Phys. Lett. B **709**, 229 (2012).
[32] Yu. Maezawa *et al*. (WHOT-QCD Collaboration), Phys. Rev. D **81**, 091501 (2010); Yu. Maezawa *et al*. (WHOT-QCD Collaboration), PoS Lattice 194 (2008).
[33] A. Nakamura, T. Saito, and S. Sakai, Phys. Rev. D **69**, 014506 (2004).
[34] A. Hart, M. Laine, and O. Philipsen, Nucl. Phys. B **586**, 443 (2000).
[35] D. Bak, A. Karch, and L. G. Yaffe, J. High Energy Phys. 08 (2007) 049 .
[36] M. Djordjevic, Phys. Rev. C **74**, 064907 (2006).
[37] M. Gyulassy, P. Levai, and I. Vitev, Phys. Lett. B **538**, 282 (2002).
[38] S. Wicks, W. Horowitz, M. Djordjevic, and M. Gyulassy, Nucl. Phys. A **784**, 426 (2007).
[39] M. Cacciari, P. Nason, and R. Vogt, Phys. Rev. Lett. **95**, 122001 (2005).
[40] M. L. Mangano, P. Nason, and G. Ridolfi, Nucl. Phys. B **373**, 295 (1992).
[41] I. Vitev and M. Gyulassy, Phys. Rev. Lett. **89**, 252301 (2002).
[42] Note that suppression results are expected to be robust with respect to the precise form of the production and fragmentation functions [45].
[43] R. Vogt, Int. J. Mod. Phys. E **12**, 211 (2003).
[44] H. L. Lai (CTEQ Collaboration), Eur. Phys. J. C **12**, 375 (2000).
[45] S. Wicks, Ph.D. thesis, Columbia University, USA, 2008.
[46] A. Dainese, Eur. Phys. J. C **33**, 495 (2004).
[47] M. Djordjevic, M. Gyulassy, and S. Wicks, Phys. Rev. Lett. **94**, 112301 (2005).
[48] M. Djordjevic and U. Heinz, Phys. Rev. C **77**, 024905 (2008).
[49] M. Djordjevic and M. Gyulassy, Phys. Rev. C **68**, 034914 (2003).
[50] G. D. Moore and D. Teaney, Phys. Rev. C **71**, 064904 (2005).
[51] P. Arnold, G. D. Moore, and L. G. Yaffe, J. High Energy Phys. 11 (2001) 057; 06 (2002) 030; 01 (2003) 030.
[52] M. Djordjevic, Nucl. Phys. A **783**, 197 (2007).
[53] I. Vitev and B. W. Zhang, Phys. Rev. Lett. **104**, 132001 (2010).
[54] A. Buzzatti and M. Gyulassy, Phys. Rev. Lett. **108**, 022301 (2012).
[55] G. Y. Qin, J. Ruppert, C. Gale, S. Jeon, G. D. Moore, and M. G. Mustafa, Phys. Rev. Lett. **100**, 072301 (2008).
[56] I. Vitev, Phys. Lett. B **606**, 303 (2005).
[57] A. Adil and M. Gyulassy, Phys. Lett. B **602**, 52 (2004).
[58] C. Peterson and D. Schlatter, I. Schmitt, and P. M. Zerwas, Phys. Rev. D **27**, 105 (1983).